

THE EFFECT OF PH ON THE FORMATION OF NICKEL NANOSTRUCTURES BY CHEMICAL REDUCTION METHOD

Mohd Ridhwan bin Ramdzan and Che Rozid bin Mamat

Department of Chemistry, Faculty of Science, Universiti Teknologi Malaysia, 81310 Johor Bahru

Abstract

The synthesis of nickel (Ni) nanostructures through chemical reduction method using hydrazine ($\text{N}_2\text{H}_4 \cdot 6\text{H}_2\text{O}$) as a reducing agent is reported. It was found the ratio of 6.65 of NaOH over NiCl_2 is necessary for the formation of pure nickel nanoparticles. NaOH was used to control the pH of solutions. Field Emission Scanning Electron Microscopy (FESEM) revealed that by varying $[\text{OH}^-]/[\text{Ni}^{2+}]$ molar ratio, various types of Ni nanostructures with size between 20 to 800 nm are obtained. Changing the pH from 8.7 to 9.5 resulted in formation of Ni wool-like nanostructure composed from chain-like nanostructure particles. The presence of nickel nanoparticles was confirmed with phase analysis using X-ray diffraction (XRD). Results show that the formation of pure Ni metal nanoparticles of wool-like nanostructure only occur when $[\text{OH}^-]/[\text{Ni}^{2+}]$ molar ratio was tailored to higher than four.

Keywords: chain-like, wool-like, nickel, nanostructures, nanoparticles

INTRODUCTION

Fascinating shapes and morphologies of nanoscale materials such as nanoparticles, nanorod, nanochain, nanocubes are among the most emerging classes of engineering materials due to its promising application in numerous technological and highly demanding fields such as sensing, biomedical, automotive, electronics, etc. [1-3]. Shape and size have been identified to have close relationship with chemical and physical properties of nanoscale materials. In some cases new properties are realized. The ability to produce nanoscale materials in various shapes and morphologies is becoming the key for further development of nanotechnology.

Pure bulk Ni is a lustrous white, hard and one of the four ferromagnetic elements at room temperature in transition metal group VIII of the Periodic Table. It has high ductility, good thermal conductivity, high strength and fair electrical conductivity. Ni nanoscale materials have received enormous attention due to their unique property in magnetic, thermal, electrical and chemical. It has been proven to have tremendous capability as catalyst, supercapacitor, additives in oil, magnetic carriers for biomedical and others [1,4-6]. Recently, synthesis of Ni in unique morphologies has becoming an interesting research because of the potential improvement of properties such as in chemical, electrical and magnetic. In some cases the new shape and morphologies create new properties which are differing when they are in spherical shape. Ni has been synthesized in various morphologies for instant, nanocubes, nanowires, flower-like, sea urchin-like and bowl-like [7-11].

In the synthesis of nanoscale materials, bottom-up approach is the most commonly used method. Bottom-up approach is a piecing together of system to a bigger system which usually involve chemical reaction such as wet chemical synthesis. Chemical reaction method has been extensively used as the synthetic method of producing nanomaterials with an advantage of more controllable of as-synthesized products. Utilizing this method, the preparation of nanoparticles can be achieved through various methods. Typical preparation chemical reaction method for Ni nanoscale materials includes polyol, microemulsion, microwave assisted and sol-gel [12-15]. Chemical reaction method requires consideration of several synthetic parameters for instant temperature, reaction time, reactants concentration etc. Wu et al. (2003) reported that Ni nanoparticles can only be obtained with appropriate amount of NaOH.

Ni nanostructure is structures that consist of Ni nanoparticles usually spherical in shape that self-assemble to form new structures. This unique phenomenon of self-assemblies, act differently depending on method of preparations. Under certain environment Ni nanoparticles tend to form secondary particles which are the results of van der Waals attractive forces and magnetic dipole interactions as well as thermodynamic driving force [17,18]. Different morphologies of nanoscale materials are normally associate with growth orientation direction. Chen et al. (2012) discovered that flower-like Ni structure is actually composed of sword-like petal particles that grows along (011) direction [19].

This work reports the effect of the pH to the shape and morphologies of as-synthesized particles by tailoring $[\text{OH}^-]/[\text{Ni}^{2+}]$ molar ratios using chemical reduction method. Investigation on the effect of pH on its shape and morphology will also be reported.

EXPERIMENTAL

Materials

All reagents are analytical grade and are used as received. Hydrazine hydrate 50% v/v, nickel chloride $\text{NiCl}_2 \cdot 6\text{H}_2\text{O}$ and sodium hydroxide powder NaOH are bought from Sigma- Aldrich company.

Preparation of Ni nanoparticles

To prepare the Ni nanoparticles, chemical reduction method of nickel salt (NiCl_2) by strong reducing agent, hydrazine hydrate in the aqueous solution are used due to better structural control on the microscopic level and low reaction temperature. The molar ratio of $\text{N}_2\text{H}_4/\text{Ni}^{2+}$ poured is 4.5 whereas that of $\text{NaOH}/\text{Ni}^{2+}$ is 2.66.

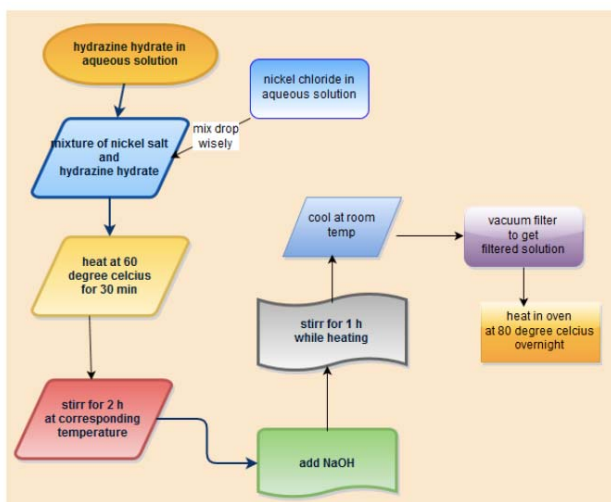
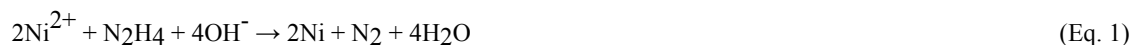


Figure 1: Process of synthesizing nickel nanoparticles product.

To be precise, 0.2 molar nickel chloride (NiCl_2) solutions are produced by diluting 0.5 g of nickel chloride solid salt with 10.517 mL of deionised water in a 25 mL beaker. 0.9 molar hydrazine hydrate (N_2H_4) are produced by diluting 2.12 mL N_2H_4 of 50% v/v concentration, 2.13 gcm^{-3} density, 40 gmol^{-1} with deionised water to make it 25 mL of solution in 50 mL beaker. The determining factor in producing nickel nanoparticle size is the amount of basic sodium hydroxide (NaOH) to alter reaction pH. 0.532 molar NaOH solutions are prepared by diluting 0.4 g NaOH powder with deionised water and are made to have 18.8 mL of NaOH solution in a 25 mL beaker. Second NaOH solution is made to increase NaOH power by 0.2 g to increase pH properties. The addition of 0.2 g NaOH powder is repeated for third, fourth and fifth solution.

NiCl_2 salt is mixed with deionised water in 50 mL beaker and shaken well. The salt solution is then put into 50 mL burette. Salt solution is poured drop wise from the burette into an appropriate amount of hydrazine hydrate (N_2H_4) taken into a flask of 250 mL. The solution of nickel salt and hydrazine hydrate are heated at 60°C for 30 min. The violet solution thus obtained is stirred for 2 h by using magnetic stirrer. An appropriate amount of NaOH is poured at corresponding reaction temperature and stirred again for an hour. The reduction reaction that takes place may be expressed by the following equation (Eq. 1).



The violet solution turned black in 10–15 min due to reduction reaction. The bluish- violet solution was obtained when the mixture of nickel chloride, NiCl_2 aqueous and hydrazine hydrate, N_2H_4 aqueous was heated for 30 min. The solution turns black when heated after the addition of sodium hydroxide, NaOH aqueous.



Figure 2: Bluish-violet solution

The resulting black coloured slurry is washed with deionised water repeatedly. The washing process is done in vacuum filtration filter filled with micron size filter paper before sucking process is done. The solid residue is vacuum filtered just after repeated washing with deionised water is done. Filtered nanopowder are placed in 1.5 L beaker and dried in the oven overnight at 80°C. Next day the dried powder is first crush into pieces using glass rod and taken into vial.

Characterization of Nickel nanoparticle

The particle sizes are determined by field emission scanning electron microscopy (FESEM) using a JEOL Model of JSM-6701F at 1nm (15kV) located at Institute of Ibnu Sina (IIS), Universiti Teknologi Malaysia Johor Bahru. FESEM is an ultra high resolution FESEM suitable for observation of fine structures of nickel nanoparticles.

XRD measurements are performed on a Bruker D8 Advance diffractometer which is licensed under Lembaga Perlesenan Tenaga Atom (LPTA) and is located in the Ibnu Sina Institute, Universiti Teknologi Malaysia Johor Bahru, using $\text{CuK}\alpha$ radiation ($\lambda = 0.1542 \text{ nm}$). The samples for XRD analyse is obtained by recovering the nickel nanoparticles from solution using a permanent magnet, then washing the precipitates using ethanol, and finally vacuum drying at room temperature.

RESULTS AND DISCUSSION

Formation of Ni nanoparticles

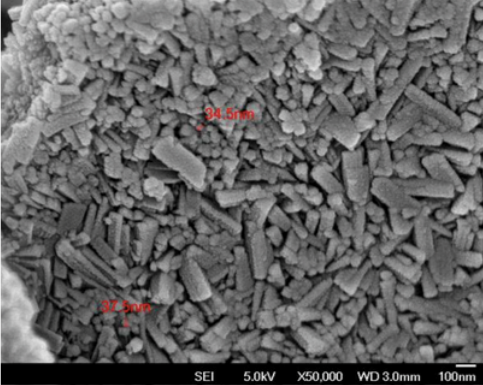
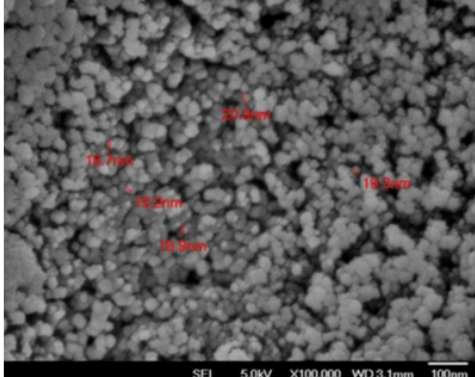
It is found that the addition of trace NaOH solution is necessary for the formation of pure nickel nanoparticles in an optimum reaction temperature of 60°C which is quite helpful in accelerating the reaction rate. It is found that the formation of nickel nanoparticles might be completed within 1 h at 60°C, but the reaction is not complete at 25 °C, even after 2 weeks. Therefore, the reaction temperature is set at 60-63°C in this work by using a digital hot plate to control the temperature.

The required molarity ratio of NaOH over NiCl_2 was raised from 2.66 to 6.65 by adding 1.0g of NaOH in the fourth trial as pH adjuster throughout the reduction reaction of nickel salt. The role of trace NaOH in the synthesis of Ni nanoparticles is quite interesting. The addition of trace NaOH led to the increase of solution pH from 8.7 to 9.5. It is suggested that the trace NaOH might act as a catalyst for the pure nanoparticle formation of nickel. Further investigation is necessary.

Particle size and structure Field emission scanning electron microscopy analysis (FESEM)

A typical FESEM micrograph and the size distribution for the nickel nanoparticles are shown in Table 4.1. Sample one(1) and four(4) having pH value of 8.7 and 9.5 respectively were characterized by FESEM at Institute of Ibnu Sina.

Table 1: FESEM structure and morphology sample 1 and 4.

Sample	Structure of nickel nanoparticle sample
1	
4	

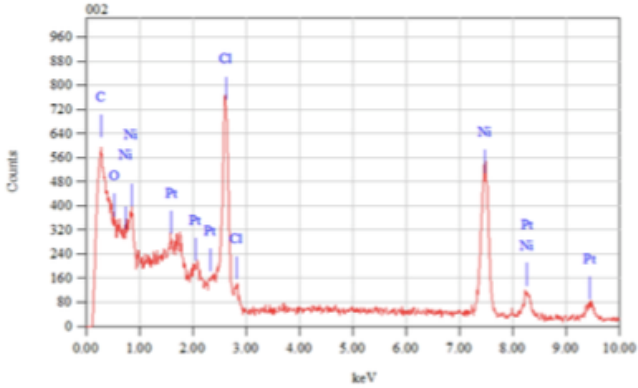
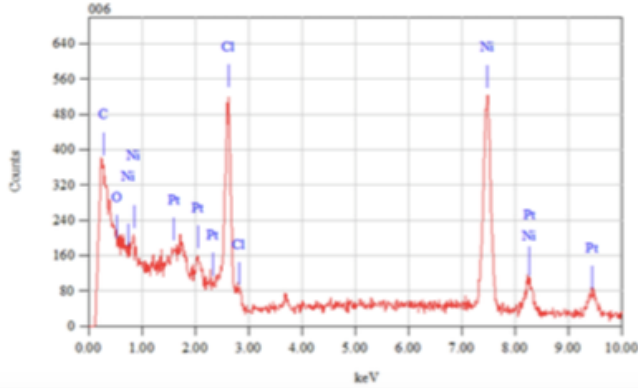
The effect of $\text{OH}^-/\text{Ni}^{2+}$ molar ratio on synthesized nanoparticles were investigated to study the effect on the reduction of Ni^{2+} ions, particles size distribution and morphology. FESEM micrographs of the particles obtained after reduction are shown in Table 1. The morphology of the starting $\text{Ni}(\text{OH})_2$ precursor (a) corresponds to long needle-like particles at 8.7 pH value. Upon reduction at higher pH value which is 9.5, the particle shape changed (b). This result correlates well with the XRD data, a clear indication that sample one(1) contains $\text{Ni}(\text{OH})_2$ precursor (i.e. elongated shape) while the Ni^0 nanoparticles is produced at higher pH value which is 9.5 for sample four(4) (i.e. round shape).

Besides, based on FESEM micrograph, higher molar ratio of $\text{OH}^-/\text{Ni}^{2+}$ of sample four(4) resulted in the formation of Ni^0 precursor with smaller size. Sample four(4) has an average particle size of 19 nm which is smaller compared to sample one(1) which having particles of 36 nm averagely. Thus, it can be concluded that higher pH value of the reaction cause the formation of smaller particles during reduction reaction.

Energy Dispersive X-ray analysis (EDX)

EDX analysis was performed for sample one(1) and sample four(4) having pH value of 8.7 and 9.5 respectively to analyse elemental composition in both samples. Peaks of elements in both sample can be seen in Table 2.

Table 2: EDX analysis of sample one(1) and sample four(4).

Sample	Structure of nickel nanoparticle sample
1	
4	

Based on EDX analysis shown above, nickel element is exist in both samples. The presence of other metal such as platinum is due to the coating purpose when doing sample preparation for FESEM and EDX analysis. Nickel counts for both sample is also the same due to the same amount of nickel chloride concentration used for nickel nanoparticles synthesis process.

The presence of chloride ion Cl^- can be observed at both samples in EDX analysis. But rather, chloride ion counts of sample four(4) is lower than sample one(1) which indicates the more successful in reduction reaction while sodium chloride, $NaCl$ solid is formed as a side product which then filter away by filter paper. Cl^- ion is still found in both sample is due to incomplete reduction reaction. This is believed due to the intensity of stirring process. The reduction reaction was performed with moderate stirring mechanism for all samples (intensity of 5 out of 10). Stronger stirring is needed to ensure complete reduction reaction. According to chemistry theory, more collision ensure better reaction which in this case is not that explain the existance of Cl^- ion in the sample.

X-ray diffraction analysis (XRD)

Sample one(1) of nickel nanopowder having 8.7 pH value is analysed by Bruker D8 Advance diffractometer using $CuK\alpha$ radiation ($\lambda = 0.1542$ nm) at 2θ in the range of 20° until 80° .

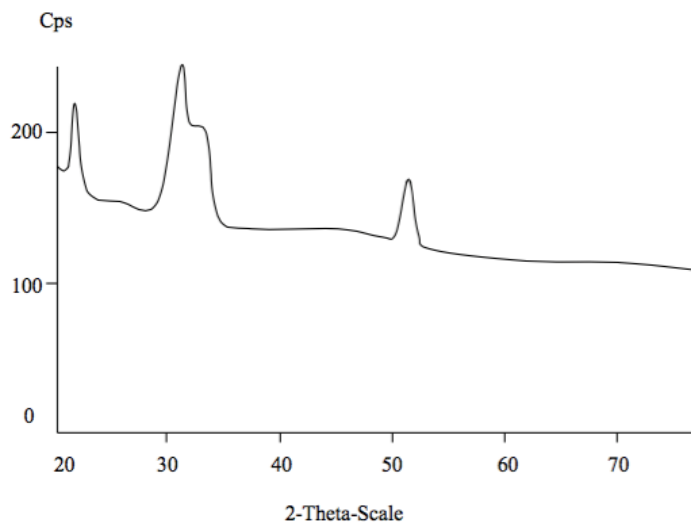


Figure 3: XRD peaks of sample one(1) at pH 8.7 (+0.0 g NaOH)

Based on the diffractogram shown above, major peaks are observed at around 21.948° and 31.337° which indicates the presence of Ni(OH)₂ precursor. Peak assigned to Ni⁰ is seen only at 51.093° having 200 crystal lattice structure.

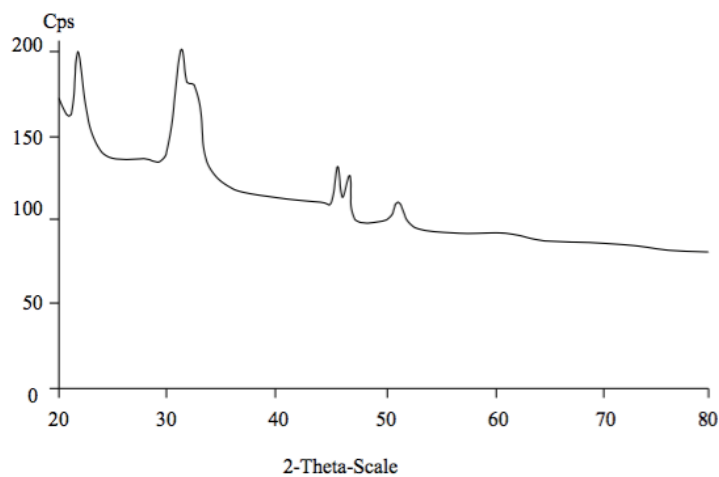


Figure 4: XRD peaks of sample four(4) at pH 9.5 (+0.6g NaOH)

Based on the spectrum above, major peaks are observed at around 21.943°, 31.235°, 32.510°, 45.445° and 51.275°. Ni(OH)₂ precursor are observed at 21.943°, 31.235° and 32.510° which are quite similar with peaks observed at sample one diffractogram. On the other hand, the peaks assigned to Ni⁰ precursor are observed for sample four(4) at diffraction line of 45.445°, 51.275°. Pure Ni⁰ was the only product observed for sample four(4), thus indicating that the reduction process leading to the formation of Ni⁰ requires higher NaOH/Ni²⁺ molar ratio.

Better Ni⁰ precursor was found in sample four(4) having 111 lattice structure. Ni⁰ precursor having 200 lattice structure is also observed in sample four(4). As a conclusion, higher pH value in sample four(4) leads to the formation of Ni⁰ precursor having 111 lattice structure. Ni⁰ precursor at 45.445° is better than Ni⁰

precursor at 51.275° due to the fact that 111 structure is higher in surface area. This criteria provide higher activity in term of catalysis in application scope.

Effects of sodium hydroxide on nickel nanoparticle crystal formation

Base on XRD spectra between sample one(1) and four(4), it is found that the addition of trace NaOH solution is necessary for the formation of pure nickel nanoparticles and an elevated reaction temperature of maximum 60oC is quite helpful in accelerating the reaction rate. It is found that the formation of nickel nanoparticles is completed within 1 h at 60oC, but the reaction is not complete at 25°C, even after 2 weeks. No nickel nanoparticle formation will happen even after one month of heating at 25°C.

Besides, adding extra NaOH molarity affect the formation of nickel nanoparticles precursor. This can be observed on the differences of sample four(4) and sample one(1) diffractograms. Sample four(4) contain diffraction lines of Ni⁰ precursor while non is observed on sample one(1) diffractogram. It can be concluded that NaOH plays an important role in forming pure nickel nanoparticle formation and also as pH adjuster throughout the reaction.

CONCLUSION

Nickel nanoparticles have been synthesized by the hydrazine reduction of nickel chloride at 60°C without soluble polymer as a protective agent. It is found that the addition of trace NaOH is necessary to form pure nickel nanoparticles precursor. The resultant particles have been characterized to be nickel amorphous structure by XRD. Nickel nanoparticle size is observed by FESEM to be around 36nm in sample one while 20 nm in sample four. The determining factor is the molarity of NaOH which identify NaOH is crucial to enhance the reaction rate thus forming difference nanostructures at difference pH. At 9.5 pH value of higher NaOH/Ni²⁺, FESEM reveals the existance of 111 Ni⁰ precursor. Stirring intensity also affect the reduction reaction in producing nickel nanoparticles.

REFERENCES

1. Stixrude, Lars; Wasserman, Evgeny; Cohen, Ronald (November 1997). "Composition and temperature of Earth's inner core". *Journal of Geophysical Research (American Geophysical Union)* 102 (B11): 24729–24740.
2. Derek G. E. Kerfoot (2005), "Nickel", *Ullmann's Encyclopedia of Industrial Chemistry*, Weinheim: Wiley-VCH, doi:10.1002/14356007.a17_157
3. Kittel, Charles. (1996). *Introduction to Solid State Physics*. Wiley. p. 449.
4. Keith Lascelles, Lindsay G. Morgan, David Nicholls, Detmar Beyersmann "Nickel Compounds" in *Ullmann's Encyclopedia of Industrial Chemistry 2005*, Wiley-VCH, Weinheim. doi:10.1002/14356007.a17_235.pub2
5. Greenwood, Norman N.; Earnshaw, Alan (1997). *Chemistry of the Elements* (2nd ed.). Butterworth-Heinemann. ISBN 0080379419.
6. Kuck, Peter H. "Mineral Commodity Summaries 2012: Nickel" (PDF). United States Geological Survey. Retrieved November 19, 2008.
7. Kuck, Peter H. "Mineral Yearbook 2006: Nickel" (PDF). United States Geological Survey. Retrieved November 19, 2008.
8. Davis, Joseph R (2000). "Uses of Nickel". *ASM Specialty Handbook: Nickel, Cobalt, and Their Alloys*. ASM International. p. 7–13.
9. Keith Lascelles, Lindsay G. Morgan, David Nicholls, Detmar Beyersmann "Nickel Compounds" in *Ullmann's Encyclopedia of Industrial Chemistry 2005*, Wiley-VCH, Weinheim.
10. Baucom, E. I.; Drago, R. S. (1971). "Nickel(II) and nickel(IV) complexes of 2,6- diacetylpyridine dioxime". *Journal of the American Chemical Society* 93 (24): 6469.
11. Mond, L.; Langer, K.; Quincke, F. (1890). "Action of carbon monoxide on nickel". *Journal of the Chemical Society* 57: 749–753.
12. Faraday, M. (1857) *Philos. Trans. R. Soc. London* , 147 , 145 – 181.
13. Turkevich, J., Stevenson, P.C., and Hillier, J. (1951) *Discuss. Faraday Soc.* 11, p. 55 – 75.
14. Rheenen, P.R.V., McKelvy, M.J., and Glaunsinger, W.S. (1987) *J. Solid State Chem.* 67, p. 151–169.
15. Henglein, A. (1989) *Chem. Rev.* , 89 , p. 1861 – 1873.
16. Burda, C., Chen, X., Narayanan, R., and El-Sayed, M.A. (2005) *Chem. Rev.* , 105 , p. 1025 – 1102.
17. Liz-Marzán, L.M. (2006) *Langmuir* , 22 , p. 32 – 41.
18. Sugimoto, T. (2000) *Fine Particles: Synthesis, Characterization, and Mechanisms of Growth*, *Surfactant Sci. Series Vol. 92*, Marcel Dekker Inc., New York.
19. Lea, M.C. (1889) *Am. J. Sci.*, 37, p. 476 – 491.

20. Yamaguchi, Y. (2008) Kagakukougaku, 72, p. 344 – 348.
21. Stoeva, S., Klabunde, K.J., Sorensen, C.M., and Dragieva, I. (2002) J. Am. Chem. Soc., 124, p. 2305 – 2311.
22. Lee, S.C. (2005). Synthesis, Characterisation and Catalytic Properties of Titanium Containing Silica Aerogel. Universiti Teknologi Malaysia: Master thesis.
23. Zainal Arifin et. al. (2001). Workshop on qualitative XRD phase identification. School of Material & Mineral Resources Engineering, Engineering Campus, Universiti Sains Malaysia. p. 1-11.
24. Ekhsan, J. (2009). Effect of titanium loading on physical properties and catalytic performance of phosphate-vanadia impregnated silica. Universiti of Teknologi Malaysia: Bachelor Thesis.
25. Parida, K. M., Sahu, N., biswal, N. R., Naik, B., Prandhan, A. C. (2008). Preparation, characterisation and photocatalytic activity of sulphate-modified titania for degradation of methyl orange under visible light. Journal of Colloid and Interface Science. 318. p. 231-237.

HYDRATION AND PROPERTIES OF BLENDED CEMENT SYSTEM INCORPORATING AEROGEL

Mohd Ikram Nul Hakim Bin Baharom and Che Rozid Bin Mamat

Department of Chemistry, Faculty of Science, Universiti Teknologi Malaysia, 81310 Johor Bahru.

Abstract

The utilization of supplementary cementing materials (SCMs) to produce economical cement that is cheaper and greener is an ongoing issue. The objectives of this study are to determine the effect of SCMs on the hydration and properties of blended cement. In this study, OPC was improvised by addition of GGBS and RHA with different weight percentages. Both types of respective were added with 1%, 2% and 3% of aerogel to improve its strength and hydrated for 7 and 28 days. The specimens were characterized by using compressive strength test, FTIR, FESEM, XRD and TGA techniques. The compressive strength test shows all specimens have increase in strength for 7 and 28 days in which the composition of OPC-GGBS with 1% aerogel shows the highest compressive strength at early hydration. FTIR shows the functional group present in the OPC- GGBS-Aerogel and OPC-RHA-Aerogel blended cement which are the water lattice of CH, CSH and CASH. The hydration product formed such as CH, CSH and ettringite were observed by using FESEM having plated shaped, foil honey-comb and fine needle-like crystal structure respectively. The formation of the hydrated was confirmed by XRD technique. The TGA technique indicates that there were 3 stages of percentage decomposition of weight loss occur on both type of specimens associated with aerogel.

Keywords: SCM, GGBS, RHA

INTRODUCTION

Cement have many properties that contribute to its strength setting and quality. These properties is assessed and control by measuring the parameter involved such as compressive strength of cement , surface area, particle size distribution, fineness and mineral composition. The production of cement is very expensive nowadays. The rapid growth in construction industry increase the demand on cement production. The cement industry is considered to be one of the most energy consuming industries, with a high rate of carbon dioxide (CO₂) emissions. Every year, it is responsible for approximately 5% of the global manmade CO₂ emissions [1]. Supplementary cementing materials (SCMs) is a proven material addressing a climate change and clean air. SCMs can be divided into natural materials and artificially made which both exhibit cementitious properties [2-3]. Some of these materials are called pozzolans (natural), which by themselves do not have any cementitious properties, but when used with portland cement, react to form cementitious compounds. Artificial SCMs have been investigated before, such as fly ash, rice husk ash, and silica fume. Their utilization has been an interesting subject of research for economic, environmental and technical reasons. When different material replaced, each materials possess different chemical and mineralogical compositions as well as different particle characteristics that have various effect on the properties of cement and concrete [4].

EXPERIMENTAL

Materials

The material that used in this study were Type 1 OPC, manufactured by Tasek Cement Corporation Berhad with 340 m²/kg specific surface. GGBS with 465 m²/kg specific surface area manufactured by YTL Cement Berhad. RHA that have been burn at 650-700 °C with excess air. Aerogel was synthesized by sol gel method followed by supercritical carbon dioxide drying.

Characterization of Blended Cement

Compressive Test Machine

The mixture of different composition blended cement were prepared by 50 mm x 50 mm x 50 mm cubes. The compressive strength test was done in accordance with ASTM C109/C109M [35]. After 24 hours, the test specimens were demolded and then cured in water. Three cubic test specimens were made from each mixture, covering two different ages of 7 and 28 days.

X-Ray Diffraction (XRD)

Phase purity and crystallinity of the samples were determined by XRD using a powder diffractometer with $\text{Cu K}\alpha$ as the radiation source with $\lambda = 1.5418\text{\AA}$. The X-ray tube voltage and current were fixed at 40 kV and 40 mA, respectively. The scan step size was 2θ in the range from 5° to 80° and the reflection position and δ -spacing were calculated from the raw data using automated data analysis programs.

Fourier Transform Infrared Spectroscopy (FTIR)

KBr technique was used. About 1/100 of sample to KBr ratio was taken by using microspatula and teaspoons respectively. Next mix both thoroughly in a mortar while grinding with the pestle. A force of approximately 10 ton was applied under vacuum for 2 minutes to form transparent pellet. Then, the pellet formed was inserted in the pellet holder and go into the sample chamber. Lastly the measurement was performed and the IR spectra was observed.

Field Emission Scanning Electron Microscope with Energy Dispersive X-ray spectroscopy (FESEM-EDX)

FESEM equipped with energy dispersive X-ray spectroscopy (EDX) was used to analyze the surface morphology and elemental information of the cement paste. A small fractured sample was soaked in acetone to stop hydration and dried at 80°C for 2 h. Then the sample was coated with 20 nm of gold to make it conductive. The accelerating voltage was set at 10 kV.

Thermogravimetry Analysis (TGA/DTA)

The percentage decomposition OPC-GGBS-aerogel and OPC-RHA aerogel for 28 day was determined using TGA/DTA. The parameter used to operate the TGA was heating rate $20^\circ\text{C}/\text{min}$ under nitrogen atmosphere. The temperature range was $50\text{-}900^\circ\text{C}$.

RESULTS AND DISCUSSION

Compressive Strength Test

The compressive strength of cement paste containing OPC-GGBS-aerogel 1% was greater than others composition due to the high pozzolanic reaction at early age. But when compared to control mix at 28 days the strength of other mix was lesser, this decline was result of low pozzolanic reaction of the SCMs

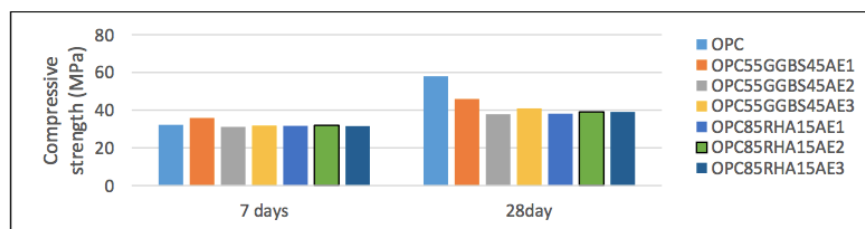


Figure 1 : Compressive strength development for 7 and 28 days

Determination of functional group in blended cement

The broad bands located at 3434 cm^{-1} and 1643 cm^{-1} are assigned to the stretching and bending vibrations of water lattice in CSH, CAH and hydrated calcium sulfoaluminates (CASH) hydrates. The band that appeared around 970 cm^{-1} is attributed to CSH.

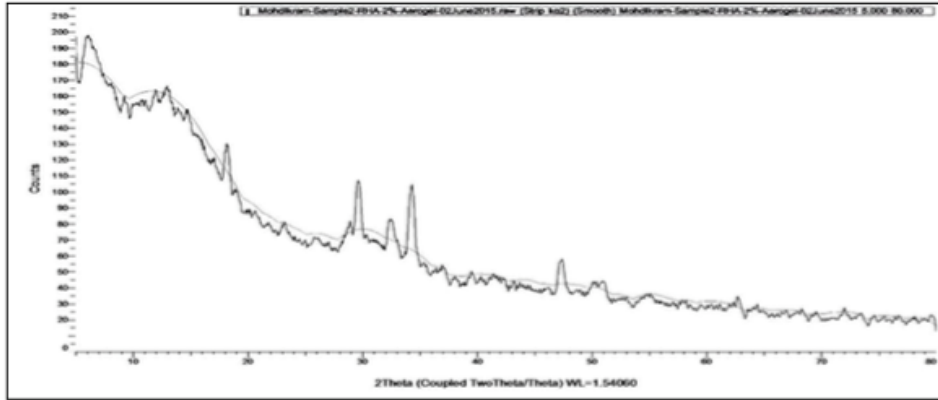


Figure 6 : OPC-RHA-Aerogel 1%

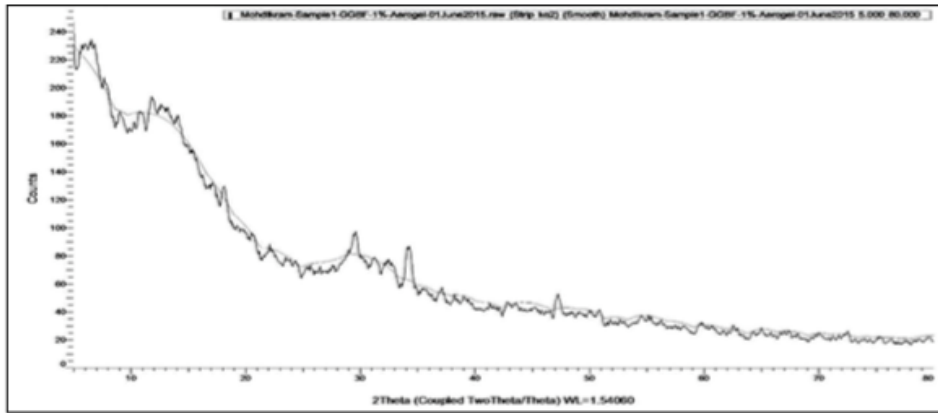


Figure 7 : OPC-GGBS-aerogel 1%

Calcium hydroxide, also known as portlandite (CH), presented at 34.259°, 18.133°, 47.358° and 34.213°, 18.133°, 47.282° in Figure 6 and Figure 7 respectively. The low intensity peak of CH in Figure 7 is due to pozzolanic reaction of the active silica and alumina of the GGBS during hydration to form CSH.

Percentage decomposition of blended cement

The first weight loss for OPC-GGBS-Aerogel 1% was lower than OPC-RHA-Aerogel 2% by 2.51%. This indicate that the amount hydrated product like water, ettringite or CSH was higher. The second weight loss is due to the decomposition of CH. Based on the table, OPC-GGBS- Aerogel 2% has the highest weight loss that is 2.74% that can relate to its strength. Due to the low third weight loss, it can be proved that OPC-RHA-Aerogel 2% has carbonate ion but the amount was low.

Table 1 : Weights loss of sample

Sample	Weight Loss (%)			
	First	Second	Third	Total
OPC-GGBS-Aerogel 1%	21.24	2.74	0.87	24.85
OPC-RHA-Aerogel 2%	23.75	1.86	0.28	25.89

CONCLUSION

The uses of SCMs have been experimentally proven to give some effect on the blended cement paste. In this study, OPC have been partially substituted with GGBS and RHA which the percentage of aerogel for both specimen were 1%, 2% and 3%. The sample were characterized by using variety of instruments. From the compressive strength test, all the specimen have increase in strength with curing time. OPC-GGBS-Aerogel 1% has higher strength at early hydration than other mix. Based on the IR spectrum, the main bands located at 3440 cm^{-1} and 1640 cm^{-1} related to the stretching and bending vibrations of water lattice in CSH, CAH and CASH.

Another main band appeared around 970 cm^{-1} which attributed to the present of CSH. It is observed from the spectrum that the hydration product are formed. In FESEM images, the structure of hydration product observed. At 28 days, a fine needle-like ettringite was observed followed by hexagonal plate-like crystal that is CH or portlandite. The CSH structure was present as foil honey-comb. In the XRD pattern fine crystalline formation was observed that are CH, CSH and C₃S. Based on the weight loss from TGA, there are 3 main decomposition occur with first decomposition are continuous weight loss start at 100-300°C followed by 450-550°C and lastly 650-900°C. CH decomposition start in the range of 450–550°C. It is proven that GGBS, RHA and addition of aerogel has pazzolanic effect in the cement paste which provide positive result on physical properties of the blended cement.

REFERENCES

1. Shen, L., Gao, T., Zhao, J., Wang, L., et al. (2014). Factory-level measurements on CO₂ emission factors of cement production in China. *Renewal. Sustainable. Energy Reviews.* 34, 337–349.
2. V. G. Papadakis, S. Tsimas. (2005). Greek supplementary cementing materials and their incorporation in concrete. *Cement & Concrete Composites.* 27, 223–230.
3. V. G. Papadakis, S. Tsimas. (2002). Supplementary cementing materials in concrete Part I: efficiency and design. *Cement and Concrete Research.* 32, 1525–1532.
4. S. Targana, A. Olgunb, Y. Erdoganb, V. Sevinc. (2002). Effects of supplementary cementing materials on the properties of cement and concrete. *Cement and Concrete Research.* 32, 1551–1558.